Structures xxx (2016) xxx–xxx

Contents lists available at ScienceDirect

Structures

journal homepage: www.elsevier.com/locate/structures

# Dynamic Time-history Elastic Analysis of Steel Frames Using One Element per Member

Si-Wei Liu *, Rui Bai, Siu-Lai Chan

*Department of Civil and Environmental Engineering, The Hong Kong Polytechnic University, Hung Hom, Kowloon, Hong Kong, China*

ARTICLE INFO

*Article history:*
Received 29 January 2016
Received in revised form 1 May 2016
Accepted 21 May 2016
Available online xxxx

*Keywords:*
Time-history
Steel
Analysis
Dynamic
Beam-column
Element
Numerical

ABSTRACT

This paper proposes an efficient numerical simulation technique for dynamic time-history analysis of space steel frames by one-element-per-member model, considering geometric nonlinearity including P-Δ-δ effects, large global deflections and member deformations. The curved arbitrarily-located-hinge (ALH) beam-column element is employed for capturing members' behaviors and simulating initial imperfections, where the internal degree-of-freedoms (DOFs) are condensed for improving the computational efficiency. The consistent element mass matrix is derived based on the Hermite interpolation function, and the Rayleigh damping model is adopted for representing the system viscosity. To solve the equation of the time-history motion, a direct time-integration method via Newmark's algorithm is utilized for the step-by-step solution. A robust numerical procedure using the incremental secant stiffness method is introduced for the large deflection analysis of space frames, allowing arbitrary rotations in a three-dimensional space. Verification examples are given to validate the present model in handling dynamic behaviors of the steel frames and members under the transient actions. The distinct feature of the research is to propose an effective analytical framework using high-performance elements, dramatically improving the numerical efficiency and making the method being practical.



## 1. Introduction

Time-history analysis is an effective simulation-based method for evaluating the structural behaviors under the transient actions, such as earthquake attacks, accidental impacts, and progressive collapse. This method is a step-by-step integration in a time domain, bringing a rational simulation of the structure subjected to the dynamic excitations. However, this procedure is usually computationally costly, mainly since a small size of time step needs to be adopted for the precision and stability in the analysis. As reported by Nguyen [1], the most time-consuming portion in the finite element analysis (FEA) algorithm is to solve the sparse, linear equations containing the tangent stiffness matrix, incremental degree-of-freedoms (DOFs) and the external force vector. For example, if a structure is modeled by two schemes, e.g. N elements with M nodes and 4N elements with 2M nodes, the size of the stiffness matrix of the latter will be four times as large as that in the former, and the calculation time increases in line with the matrix's size. Therefore, a dramatic saving on the computational expense can be achieved when fewer elements are used in a structural system.

Some researchers have utilized the nonlinear dynamic analysis method for studying the response of steel frames under the transient motions, such as Nader and Astaneh [2], Chui and Chan [3], Awkar and Lui [4], Chan and Chui [5], Gupta and Krawinkler [6], Foutch and Yun [7], Ohtori et al. [8], Silva et al. [9] and Nguyen and Kim [10] and so on. Nowadays, the time-history analysis method has already become one of the effective tools for seismic design of structures, and is codified in the modern seismic design standards, such as Eurocode 8 [11].

The prominent emphasis in designing steel members and structures is the consideration of stability problems, and thereby, second-order effects in terms of P-Δ and P-δ effects should be properly captured in analysis. Global frame and local member imperfections should be necessarily taken into account, otherwise, the factors of instability lying in the structural system and the members cannot be effectively detected. Frame imperfection is usually applied according to the Eigen-buckling mode shapes [12], while the local member imperfection is simulated using a sine curve (see Fig. 1). The conventional method adopts several straight elements to represent the imperfection, and it causes extra manipulating efforts in offsetting the nodes. To this end, one-element-per-member model is employed in the present study, not only the computer time can be dramatically reduced, but also does it bring convenience in modeling the initial member imperfections according to the requirements in the modern design codes. This research aims to extend the application of this analytical model to the dynamic time-history analysis for seismic design.

Therefore, the selection of a beam-column element, which should be initially curved and can simulate large deformation in an element, is vital and essential for a successful analysis using a one-element-per-member model. Therefore, several sophisticated elements have been developed in the recent decade, especially aiming for simulating slender members with imperfections. The Pointwise-Equilibrium-Polygonal (PEP) beam-column element with the high-order shape function is derived by Chan and Zhou [13], and has been extensively adopted in the practice over the past 16 years. Subsequently, Chan and Gu [14]

* Corresponding author. Tel.: +852 2334 6389; fax: +852 2334 6389.
*E-mail address:* siwei.liu@connect.polyu.hk (S.-W. Liu).

http://dx.doi.org/10.1016/j.istruc.2016.05.006
2352-0124/

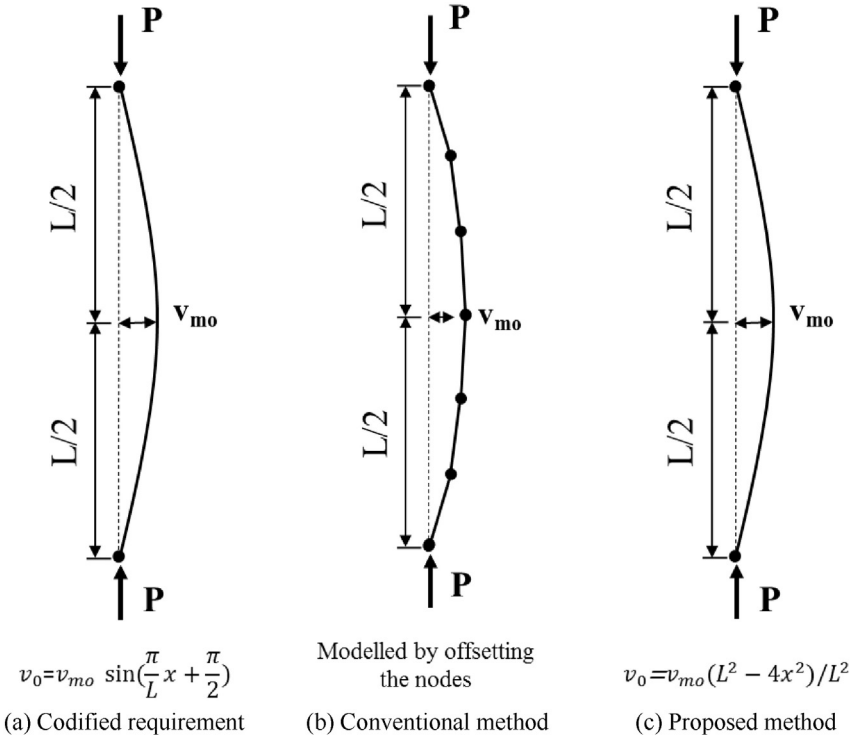


**Fig. 1.** Modeling of initial member imperfections.

refined the classical stability function element by incorporating the member imperfections to the formulations, which is suitable for analyzing the extremely-slender columns. Recently, the Arbitrarily-Located-Hinge (ALH) element with initial curvatures has been developed by Liu et al. [15,16], being possessed of an internal node to reflect inelastic behavior and the large deformation along the member length. In the present study, the ALH element is employed and extended its application to the dynamic time-history elastic analysis of steel frames.

Two main approaches are popularly utilized for solving the structural dynamic problems [17], e.g. response spectrum and time-history analysis methods. The former approach provides an approximated solution to estimate the peak values of displacements and forces for a system, ignoring all the nonlinear effects, e.g. geometric and material nonlinearities. This method is usually adopted in the conventional design with a small-scale excitation due to its simplicity. However, in order to obtain the 'exact' time-history response of the structure at a specified moment, time history analysis method seems to be the only option. In the current study, a time integration approach using Newmark's algorithm is introduced, which is unconditionally stable numerical integration method [18] and widely adopted for solving structural dynamic problems to show its reliability and validity. For an accurate reflection of accelerated motions within members, the consistent mass matrix [17] is derived based on the Hermite interpolation function. To represent the system viscosity, an approximated method using the Rayleigh [19] damping model is adopted.

Structural members might exhibit large deformations in a nonlinear dynamic analysis. In this paper, the incremental secant stiffness method [20] based on the co-rotational description is employed for achieving arbitrarily nodal rotations during the numerical procedure. In this method, each element has its own local axes system. The element deformations and axes' rigid-body movements are separately considered, and the final nodal rotations are calculated by a gradual transformation process instead of a summation. The method has been proven to be accurate and efficient by extensive research, e.g. So and Chan [21], Ho and Chan [22], and Liu et al. [23,24].

In this paper, the element formulations, e.g. tangent stiffness, mass and damping matrixes, are derived and presented with details, and direct time-integration method using the Newmark's method is elaborated. For describing the kinematic motion of elements during the incremental-iterative procedure, the incremental secant stiffness approach is introduced. Finally, several examples are given for the verifications and validations.

## 2. Assumptions

The following assumptions are taken in the deriving the element formulations and given as: (1) the Euler–Bernoulli's assumption is made, where the plan section before and after deformations are kept being normal to the centroid axes; (2) strains assume to be small, while the displacements and rotations can be arbitrarily large, using the incremental secant stiffness method [25]; (3) material's behavior is assumed to be elastic throughout the whole analysis procedure; (4) warping and shear deformations are not included in the element formulations; and (5) the applied forces are conservative and added to the nodes, remaining to be independent of the loading history.

## 3. Element formulations

To capture reliably the structural behavior under loads, the influential effects inherent to the beam-column members are considered, and namely they are the initial imperfections, large deflection and P-δ effect and so on. The arbitrarily-located-hinge (ALH) element proposed by Liu et al. [15,16] is used in the present study. This element explicitly simulates the initial member curvatures, and it is also capable of modeling the large member deformation by one element. A review of the ALH element is presented herein, and detailed formulations should be referred to the original paper proposed by Liu et al. [15,16]. Furthermore, the mass and damping matrixes for the ALH element are derived in this section.

Please cite this article as: Liu S-W, et al, Dynamic Time-history Elastic Analysis of Steel Frames Using One Element per Member, Structures (2016), http://dx.doi.org/10.1016/j.istruc.2016.05.006

### 3.1. Shape functions with the initial member imperfections

There are twelve degrees of freedoms (DOFs) in an element as shown in Fig. 2. Expressing the relations to the lateral displacement, we have,

$$v_y = \begin{cases} \{N_{11}\ N_{12}\ N_{13}\} \cdot \{\theta_{11y}\ \theta_{12y}\ \delta_z\}^T \\ \{N_{21}\ N_{22}\ N_{23}\} \cdot \{\theta_{21y}\ \theta_{22y}\ \delta_z\}^T \end{cases} \text{ and } \begin{matrix} -L/2 \le x \le \xi L \\ \xi L \le x \le L/2 \end{matrix} \quad (1)$$

$$v_z = \begin{cases} \{N_{11}\ N_{12}\ N_{13}\} \cdot \{\theta_{11z}\ \theta_{12z}\ \delta_y\}^T \\ \{N_{21}\ N_{22}\ N_{23}\} \cdot \{\theta_{21z}\ \theta_{22z}\ \delta_y\}^T \end{cases} \text{ and } \begin{matrix} -L/2 \le x \le \xi L \\ \xi L \le x \le L/2 \end{matrix} \quad (2)$$

where, $L$ is the length of the member; $x$ is coordinates in the local element axes; $\xi$ is the non-dimensional coordinates of the internal hinge; $v_y$ and $v_z$ are the lateral displacement functions along y-axis and z-axis, respectively; $\theta_{11y}$, $\theta_{11z}$, $\theta_{22y}$ and $\theta_{22z}$ are the external rotations at ends about two principal axes; $\delta_y$, $\delta_z$, $\theta_{12y}$, $\theta_{12z}$, $\theta_{21y}$ and $\theta_{21z}$ are the internal lateral deflections and rotations at two principal axes; and $N_{11}$, $N_{12}$, $N_{13}$, $N_{21}$, $N_{22}$ and $N_{23}$ are shape parameters for the shape functions writing as:

$$N_{11} = \frac{2(L+2x)(x-L\xi)^2}{L^2(1+2\xi)^2} \quad (3)$$

$$N_{12} = \frac{(L+2x)^2(x-L\xi)}{L^2(1+2\xi)^2} \quad (4)$$

$$N_{13} = \frac{(L+2x)^2(L-4x+6L\xi)}{L^3(1+2\xi)^3} \quad (5)$$

$$N_{21} = \frac{(L-2x)^2(x-L\xi)}{L^2(1-2\xi)^2} \quad (6)$$

$$N_{22} = -\frac{2(L-2x)(x-L\xi)^2}{L^2(1-2\xi)^2} \quad (7)$$

$$N_{23} = \frac{(L-2x)^2(L+4x+6L\xi)}{L^3(1-2\xi)^3} \quad (8)$$

The initial member imperfection is explicitly modeled by a parabolic equation as,

$$v_{0y} = v_{moy}\left(L^2-4x^2\right)/L^2 \quad -L/2 \le x \le L/2 \quad (9)$$

$$v_{0z} = v_{moz}\left(L^2-4x^2\right)/L^2 \quad -L/2 \le x \le L/2 \quad (10)$$

where $v_0$ is the shape function of initial member imperfection; $v_{mo}$ is the amplitude of initial member curvature at the mid-span and usually set to be the values given in the modern design codes like Eurocode 3 [12].

Reflecting the bowing effect due to bending is crucial for the analysis method by one element per member and this can be computed as,

$$u_b = \frac{1}{2}\int_L \left(\dot{v}_y{}^2 + 2v_{\dot{o}y}\dot{v}_y\right)dx + \frac{1}{2}\int_L \left(\dot{v}_z{}^2 + 2v_{\dot{o}z}\dot{v}_z\right)dx \quad (11)$$

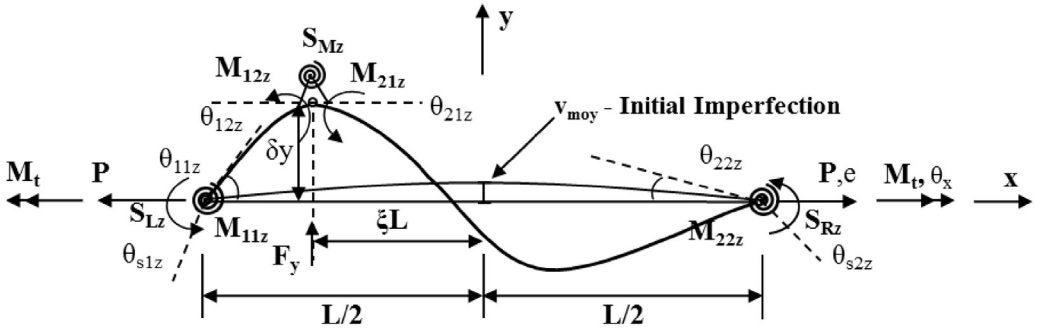


(a) Along y-axis

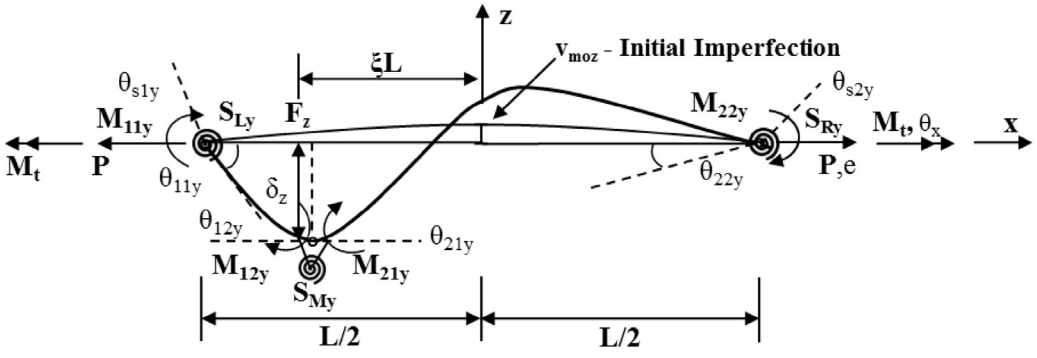


(b) Along z-axis

**Fig. 2.** Local member basic forces and deformations.

Please cite this article as: Liu S-W, et al, Dynamic Time-history Elastic Analysis of Steel Frames Using One Element per Member, Structures (2016), http://dx.doi.org/10.1016/j.istruc.2016.05.006

### 3.2. Secant relations for resisting forces

In order to obtain the resisting forces in the incremental-iterative procedure, the secant relations are required and can be obtained by formulating the total potential energy of an element written as,

$$U=\frac{1}{2}\int_L EA\dot{u}^2dx+\frac{1}{2}\int_L EI_y\ddot{v}_y{}^2dx+\frac{1}{2}\int_L EI_y\ddot{v}_z{}^2dx+\frac{1}{2}\int_L GJ\dot{t}^2dx +\frac{1}{2}\int_L P\left(\dot{v}_y{}^2+2\dot{v}_{oy}\dot{v}_y\right)dx+\frac{1}{2}\int_L P\left(\dot{v}_z{}^2+2\dot{v}_{0z}\dot{v}_z\right)dx+\int_{\theta_{my}} S_{my}d\theta+\int_{\theta_{mz}} S_{mz}d\theta \tag{12}$$

where, $EA$ is the axial rigidity along x axis; $EI_y$ and $EI_z$ are the flexural rigidities about y- and z- axes respectively; $GJ$ is the torsional rigidity; $\theta_{my}$, $\theta_{mz}$, $S_{my}$ and $S_{mz}$ are the hinge rotations and stiffness at middle hinge about the y- and the z- axes respectively.

Since the present study focuses on the elastic response of the structure, the plastic deformations of the element are fully restrained by assuming the stiffness of the hinge to be infinitely large. Furthermore, to simplify the element formulations for the use in an elastic analysis, the internal node is fixed at the mid-span. Thus, the secant relations can be rewritten and given in the Appendix I.

### 3.3. Tangent stiffness matrix

To predict incremental displacements due to applied an incremental forces, the tangent stiffness is required and calculated as the follows.

$$\delta^2\Pi=\frac{\partial^2\Pi}{\partial u_i\partial u_j}\delta u_i\delta u_j=\left[\frac{\partial F_i}{\partial u_j}+\frac{\partial F_i}{\partial q}\frac{\partial q}{\partial u_j}\right]\delta u_i\delta u_j \tag{13}$$

Therefore, the tangent stiffness matrix is output and written in terms of two parts as,

$$[k]_e=[k]_L+[k]_G \tag{14}$$

where, $[k]_e$ is the element tangent stiffness; $[k]_L$ is the linear stiffness matrix of an element; and $[k]_G$ is the geometric stiffness matrix of an element.

The element stiffness matrix is to be condensed to six degrees of freedom for compatibility to the common finite-element program as well as improving the numerical efficiency. The relation between the condensed stiffness matrix $[k]^*$ and the generalized force $\{f\}$ are given as,

$$\{f\}=[k]^*\{u\}_e \tag{15}$$

and,

$$[k]^*=[k]_{ee}-[k]_{ie}{}^T[k]_{ii}^{-1}[k]_{ie} \tag{16}$$

$$\{f\}=\{F\}_e-[k]_{ie}^T[k]_{ii}^{-1}\{F\}_i \tag{17}$$

also, the internal DOFs can be computed as,

$$\{u\}_i=[k]_{ii}^{-1}\left(\{F\}_i-[k]_{ie}\{u\}_e\right) \tag{18}$$

where, $\{u\}_e$ is the external DOFs and expressed as $\{e\ \ \theta_{11y}\ \ \theta_{11z}\ \ \theta_x\ \theta_{22y}\ \theta_{22z}\}^T$; $\{u\}_i$ is the internal DOFs as $\{\theta_{12y}\ \ \theta_{12z}\ \ \delta_z\ \ \delta_y\ \theta_{21y}\theta_{21z}\}^T$; $\{F\}_e$ is the force vector applied at external nodes as $\{P\ M_{11y}M_{11z}M_xM_{22y}\ M_{22z}\}^T$; and $\{F\}_i$ is the internal force vector written as $\{M_{12y}\ M_{12z}F_z\ F_yM_{21y}M_{21z}\}^T$.

When the element tangent stiffness is formulated by referring to the local axes, the global 12 by 12 element tangent stiffness matrix can be obtained using the transferring matrixes. The process is given as:

$$[\mathrm{K}]_e=[L]\left([T][k]^*[T]^T+[N]\right)[L]^T \tag{19}$$

where, $[L]$ is the transformation matrix from the member intermediate axes to global axes; $[T]$ is the transformation matrix from the member local axes to the member intermediate axes; and $[N]$ is the rigid-body movement matrix. All these matrixes can be found in the papers by Liu et al. [15,16].

Thus, the global stiffness matrix can be assembled as,

$$[\mathrm{K}]_g=\sum_1^{NELE}[\mathrm{K}]_e^i \tag{20}$$

in which, NELE notes for the total element number; and $[\mathrm{K}]_g$ is the global stiffness matrix.

### 3.4. Consistent mass matrix

Dynamic excitation force acts on the mass in a structural system, and its accuracy in a simulation is directly affected by the modeling method for the mass sources. To properly reflect the distributed mass of a member, the consistent mass matrix is derived based on the Hermite shape function given by Bathe [17], and determined as:

$$[M]_e=\int_L(v^T\rho\mathrm{A}v)dx \tag{21}$$

where, $v$ is a vector of parameters in the shape function; and $[M]_e$ is the mass matrix of the element; $\rho$ is the density of the material; and $A$ is the cross section area.

Therefore, the consistent mass matrix for an element can be formulated as below:

$$[M]_e=\frac{\rho\mathrm{AL}}{420}\begin{bmatrix}
140 & 0 & 0 & 0 & 0 & 0 & 70 & 0 & 0 & 0 & 0 & 0\\
 & 156 & 0 & 0 & 0 & 22L & 0 & 54 & 0 & 0 & 0 & -13L\\
 & & 156 & 0 & -22L & 0 & 0 & 0 & 54 & 0 & 13L & 0\\
 & & & 0 & 0 & 0 & 0 & 0 & 0 & 0 & 0 & 0\\
 & & & & 4L^2 & 0 & 0 & 0 & -13L & 0 & -3L^2 & 0\\
 & S. & & & & 4L^2 & 0 & 13L & 0 & 0 & 0 & -3L^2\\
 & & & & & & 140 & 0 & 0 & 0 & 0 & 0\\
 & & Y. & & & & & 156 & 0 & 0 & 0 & -22L\\
 & & & & & & & & 156 & 0 & 22L & 0\\
 & & & M. & & & & & & 0 & 0 & 0\\
 & & & & & & & & & & 4L^2 & 0\\
 & & & & & & & & & & & 4L^2
\end{bmatrix} \tag{22}$$

And the global mass matrix can be correspondingly assembled as:

$$[M]_g=\sum_1^{NELE}\left([L][M]_e^i[L]^T\right) \tag{23}$$

in which, $[M]_g$ is the global mass matrix.

### 3.5. Rayleigh damping matrix

An accurate simulation on the system viscosity is difficult, due to the complexity in evaluating the distributed damping coefficient per member length. In the current study, an approximated method using Rayleigh damping model [19] is adopted as expressed as below:

$$[C]_g=a[M]_g+b[K]_g \tag{24}$$

herein, $[C]_g$ is the global damping matrix; and $a$ and $b$ are the proportional coefficients for the mass and stiffness, respectively, and given as,

$$a=\frac{4\pi(\mu_1T_1-\mu_2T_2)}{\left(T_1^2-T_2^2\right)} \tag{25}$$

Please cite this article as: Liu S-W, et al, Dynamic Time-history Elastic Analysis of Steel Frames Using One Element per Member, Structures (2016), http://dx.doi.org/10.1016/j.istruc.2016.05.006

$$b = \frac{T_1 T_2(\mu_1 T_1 - \mu_2 T_2)}{\pi\left(T_1^2 - T_2^2\right)} \tag{26}$$

where, $T_1$ and $T_2$ are the natural periods at the first and second modes, respectively; and $\mu_1$ and $\mu_2$ are the damping ratios at the first and second natural modes, respectively.

## 4. Numerical algorithm using the Newmark's method

In order to solve the equations of motions in the dynamic time-history analysis, the update Lagrangian description is adopted in an incremental-iterative procedure as illustrated in Fig. 3. The numerical procedure with respect to time is in the time-domain, where the whole time history is split into many small steps with an equal time-interval Δt. And the solution for the t + Δt moment is conducted by referring to the last-known equilibrium condition at the t moment. For the step-by-step integration of the time steps, the Newmark's [18] algorithm is introduced, which is an unconditionally stable computer method with the constant-average-acceleration assumption. This method is stable, extensively accepted for solving the structural dynamic problems.

The equation of motion at the time t + Δt is conducted on the basis of the last-known confirmation at the time t, and the incremental form of the equation can be expressed as,

$$[M]_g\{\Delta\ddot{u}\} + [C]_g\{\Delta\dot{u}\} + [K]_g\{\Delta u\} = \{\Delta F\} \tag{27}$$

where, $\{\Delta u\}$, $\{\Delta\dot{u}\}$ and $\{\Delta\ddot{u}\}$ are the vectors of the nodal displacement, velocity and acceleration at a time increment; and $\{\Delta F\}$ is the incremental force vector at a time increment.

For simulating the seismic motion, the incremental force vector is written as,

$$\{\Delta F\} = -[M]_g[E]\{\Delta\ddot{x}_g\} \tag{28}$$

in which, $[E]$ is an index vector for representing the directions of the seismic motion; and $\{\Delta\ddot{x}_g\}$ is the increment of the ground acceleration.

Using the Newmark's [18] algorithm the velocity and the acceleration at the time t + Δt can be calculated as,

$$\left\{{}^{t+\Delta t}\dot{u}\right\} = \left\{{}^{t}\dot{u}\right\} + (1+\gamma)\Delta t\left\{{}^{t}\ddot{u}\right\} + \gamma\Delta t\left\{{}^{t+\Delta t}\ddot{u}\right\} \tag{29}$$

$$\left\{{}^{t+\Delta t}u\right\} = \left\{{}^{t}u\right\} + \Delta t\left\{{}^{t}\dot{u}\right\} + (1/2-\beta)\Delta t^2\left\{{}^{t}\ddot{u}\right\} + \beta\Delta t^2\left\{{}^{t+\Delta t}\ddot{u}\right\} \tag{30}$$

where, $\{{}^{t}u\}$, $\{{}^{t}\dot{u}\}$ and $\{{}^{t}\ddot{u}\}$ are the displacement, the velocity and the acceleration at the previous time t; $\Delta t$ is the constant time-interval; and $\gamma$ and $\beta$ are the Newmark factors, usually taken as 0.25 and 0.5, respectively, affect the stability and reliability in the integration method.

Therefore, the incremental equilibrium equation for calculating the displacement increment are written as,

$$[K]_{eff}\left\{{}^{t}\Delta u\right\} = [\Delta F]_{eff} \tag{31}$$

in which, $[K]_{eff}$ is the effective stiffness matrix at the time $t$; and $[\Delta F]_{eff}$ is the effective external force vector. They are expressed as,

$$[K]_{eff} = c_1[M]_g + c_4[C]_g + [K]_g \tag{32}$$

$$[\Delta F]_{eff} = \left\{{}^{t}\Delta F\right\} - (c_2[M] + c_5[C])\left\{{}^{t}\dot{u}\right\} - (c_3[M] + c_6[C])\left\{{}^{t}\ddot{u}\right\} \tag{33}$$

where, $c_1$ to $c_6$ are the factors related to the Newmark's parameters and given as,

$$c_1 = \frac{1}{\beta(\Delta t)^2} \tag{34}$$

$$c_2 = \frac{1}{\beta\Delta t} \tag{35}$$

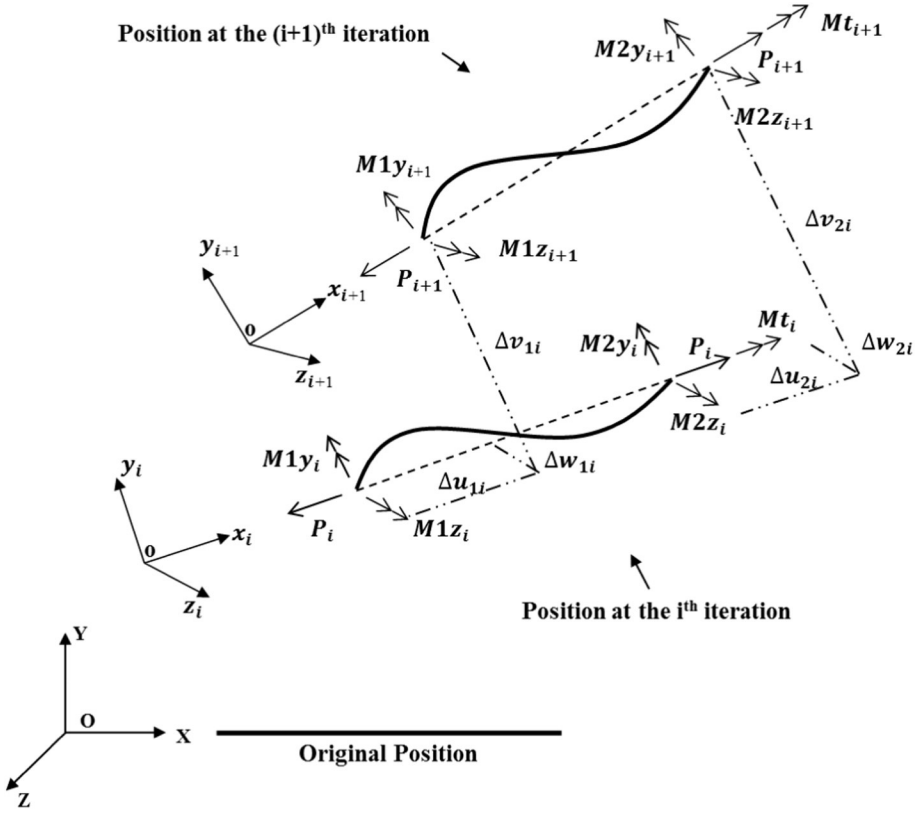


**Fig. 3.** Updated Lagrangian description in an incremental-iterative procedure.

Please cite this article as: Liu S-W, et al, Dynamic Time-history Elastic Analysis of Steel Frames Using One Element per Member, Structures (2016), http://dx.doi.org/10.1016/j.istruc.2016.05.006

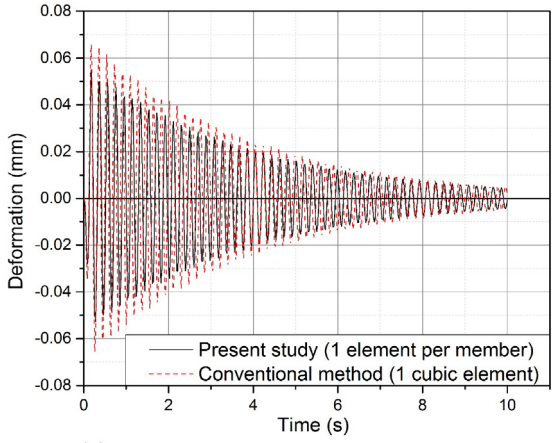


(a) Present model vs. 1 cubic element per member model

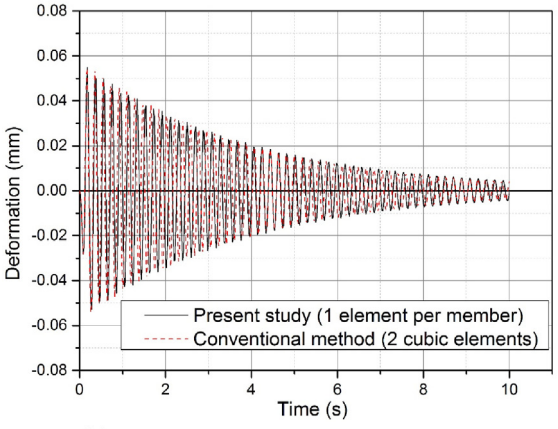


(b) Present model vs. 2 cubic elements per member model

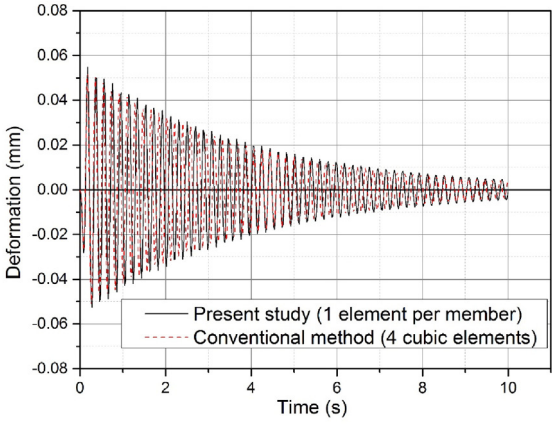


(c) Present model vs. 4 cubic elements per member model

**Fig. 4.** The comparison results of the cantilever column.

$$c_3 = -\frac{1}{2\beta} \tag{36}$$

$$c_4 = \frac{\gamma}{\beta \Delta t} \tag{37}$$

$$c_5 = -\frac{\gamma}{\beta} \tag{38}$$

$$c_6 = -\left(\frac{\gamma}{2\beta} - 1\right)\Delta t \tag{39}$$

After obtaining the displacement increment $\{^t\Delta u\}$ at the time t + Δt, the increments of velocity and acceleration can be calculated as following,

$$\{^t\Delta \dot{u}\} = c_4\{^t\Delta u\} + c_5\{^t\dot{u}\} + c_6\{^t\ddot{u}\} \tag{40}$$

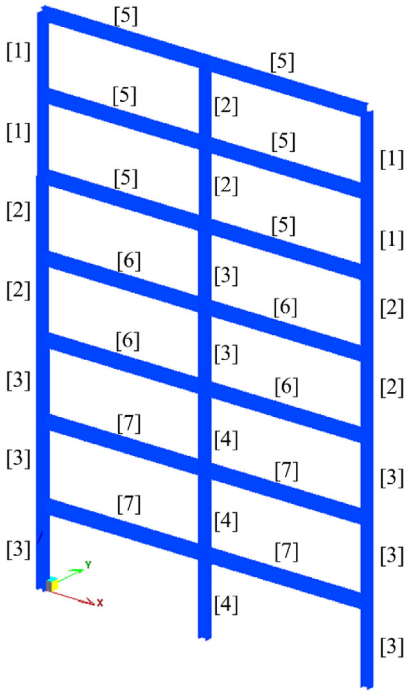


(a) Assignments of sections

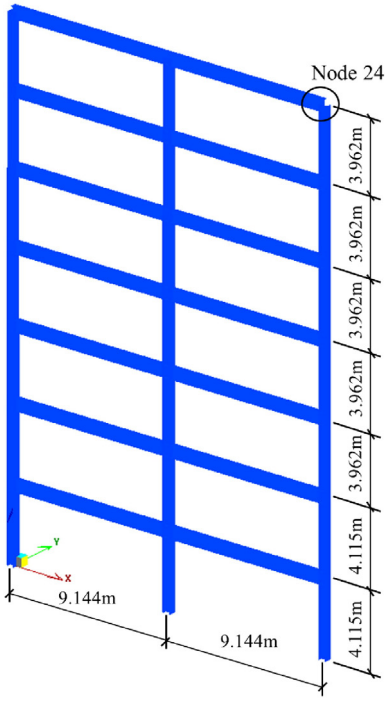


(b) Dimensions

**Fig. 5.** Configuration of the seven-story frame.

Please cite this article as: Liu S-W, et al, Dynamic Time-history Elastic Analysis of Steel Frames Using One Element per Member, Structures (2016), http://dx.doi.org/10.1016/j.istruc.2016.05.006

**Table 1**
Section ID and properties in the planar frame.

| ID | Section name | Width | Depth | Web thickness | Flange thickness |
|---|---|---|---|---|---|
| | | mm | mm | mm | mm |
| 1 | W14x176 | 398.78 | 386.08 | 21.08 | 33.27 |
| 2 | W14x211 | 401.32 | 398.78 | 24.89 | 39.62 |
| 3 | W14x257 | 406.40 | 416.56 | 29.97 | 48.01 |
| 4 | W14x283 | 408.94 | 424.18 | 32.77 | 52.58 |
| 5 | W14x117 | 325.12 | 617.22 | 13.97 | 21.59 |
| 6 | W14x131 | 327.66 | 622.30 | 15.37 | 24.38 |
| 7 | W14x126 | 330.20 | 635.00 | 17.91 | 30.99 |

$$\{{}^t\Delta\ddot{u}\} = c_1\{{}^t\Delta u\} + c_1\{{}^t\dot{u}\} + c_3\{{}^t\ddot{u}\} \tag{41}$$

Therefore, the models are updated, including the geometry, displacement, velocity, acceleration and total applied forces, using the following equations,

$$\{{}^{t+\Delta t}x\} = \{{}^t x\} + \{{}^t\Delta u\} \tag{42}$$

$$\{{}^{t+\Delta t}u\} = \{{}^t u\} + \{{}^t\Delta u\} \tag{43}$$

$$\{{}^{t+\Delta t}\dot{u}\} = \{{}^t\dot{u}\} + \{{}^t\Delta\dot{u}\} \tag{44}$$

$$\{{}^{t+\Delta t}\ddot{u}\} = \{{}^t\ddot{u}\} + \{{}^t\Delta\ddot{u}\} \tag{45}$$

$$\{{}^{t+\Delta t}F\} = \{{}^t F\} + \{{}^t\Delta F\} \tag{46}$$

To check the equilibrium condition, the unbalanced forces are computed as,

$$\{{}^t\Delta F^*\} = \{{}^{t+\Delta t}F\} - \left([M]_g\{{}^{t+\Delta t}\ddot{u}\} + [C]_g\{{}^{t+\Delta t}\dot{u}\} + \{{}^{t+\Delta t}R\}\right) \tag{47}$$

Accordingly, an residual displacement due to the unbalanced forces is calculated as,

$$\{{}^t\Delta u\}_i = [K]_{eff}^{-1}\{{}^t\Delta F^*\} \tag{48}$$

And the convergence criterions in terms of residual displacement and forces are determined as below,

$$\frac{\{{}^t\Delta u\}_i^T\{{}^t\Delta u\}_i}{\{{}^{t+\Delta t}u\}_i^T\{{}^{t+\Delta t}u\}_i} < TOL \tag{49}$$

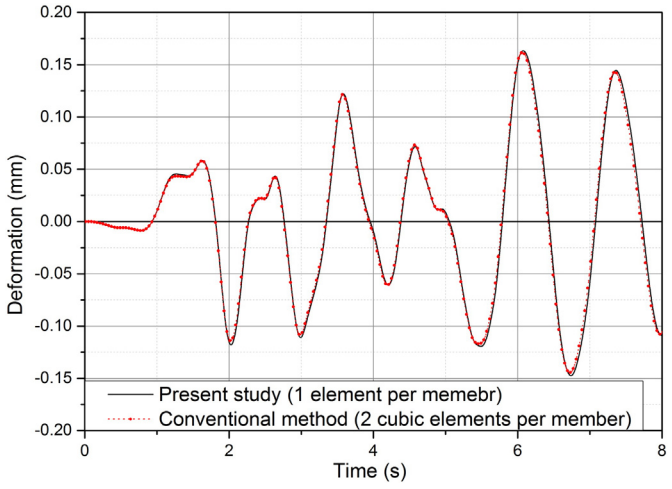


**Fig. 6.** The comparisons results of the seven-story frame.

$$\frac{\{{}^t\Delta F^*\}_i^T\{{}^t\Delta F^*\}_i}{\{{}^{t+\Delta t}F\}_i^T\{{}^{t+\Delta t}F\}_i} < TOL \tag{50}$$

in which, TOL is the tolerance for the numerical iteration, and usually taken as 0.1%.

If the convergence criterions are not satisfied, the residual displacement is used to update the model as,

$$\{{}^{t+\Delta t}x\}_{i+1} = \{{}^{t+\Delta t}x\}_i + \{{}^t\Delta u\}_i \tag{51}$$

$$\{{}^{t+\Delta t}u\}_{i+1} = \{{}^{t+\Delta t}u\}_i + \{{}^t\Delta u\}_i \tag{52}$$

$$\{{}^{t+\Delta t}\dot{u}\}_{i+1} = \{{}^{t+\Delta t}\dot{u}\}_i + c_4\{{}^t\Delta u\}_i \tag{53}$$

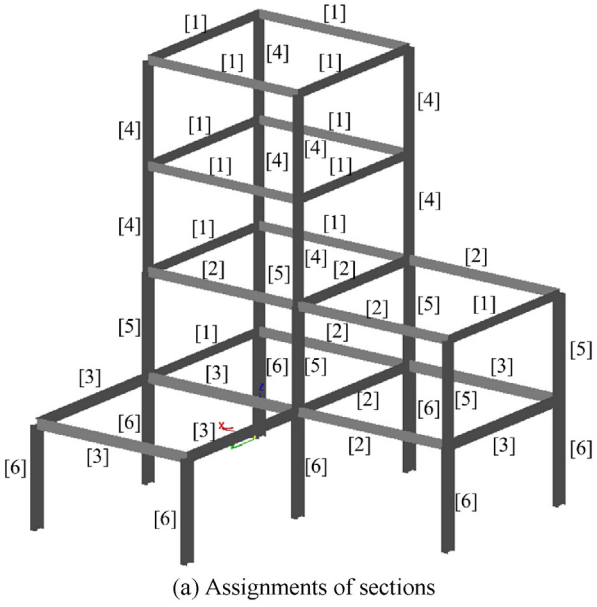

(a) Assignments of sections

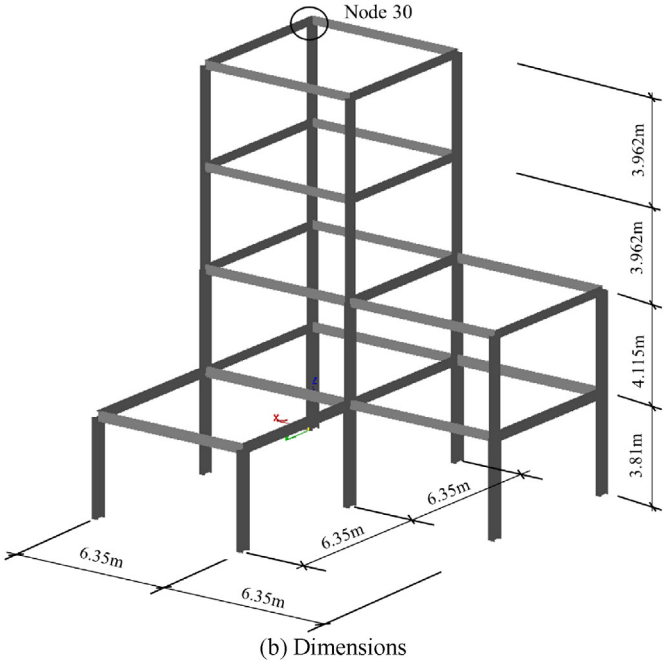


(b) Dimensions

**Fig. 7.** The configuration and dimensions of the 3D frame.

Please cite this article as: Liu S-W, et al, Dynamic Time-history Elastic Analysis of Steel Frames Using One Element per Member, Structures (2016), http://dx.doi.org/10.1016/j.istruc.2016.05.006

**Table 2**
Section ID and properties in the spatial frame.

| ID | Section name | Width | Depth | Web thickness | Flange thickness |
|---|---|---|---|---|---|
| | | mm | mm | mm | mm |
| 1 | W12x16 | 101.35 | 304.80 | 5.59 | 6.73 |
| 2 | W12x30 | 165.61 | 312.42 | 6.60 | 11.18 |
| 3 | W14x30 | 170.94 | 350.52 | 6.86 | 9.78 |
| 4 | W14x53 | 204.72 | 353.06 | 9.40 | 16.76 |
| 5 | W14x82 | 256.54 | 363.22 | 12.95 | 21.72 |
| 6 | W16x67 | 259.08 | 414.02 | 10.03 | 16.89 |

$$\{^{t+\Delta t}\ddot{u}\}_{i+1} = \{^{t+\Delta t}\ddot{u}\}_i + c_1\{^t\Delta u\}_i \tag{54}$$

The above iterative procedure is repeated till the convergence criterions are satisfied.

## 5. Incremental secant stiffness method

The incremental stiffness method on the basis of the updated Lagrangian description is adopted for updating the model in the incremental-iterative procedure. In this method, the equilibrium conditions are determined by referring to the last-known configuration. The method has been proven to be efficient and effective by many researchers. For example, Chan [26] used this method for inelastic analysis of the tubular member. Yang and Chiou [27] adopted the method to analyze the planer frame. Argyris [28] used this approach to study the three-dimensional frame.

At each load increment, the analysis is to calculate the resisting forces at the $i+1$th position by referring to the last-known configuration at the $i$th position (see Fig. 3). The incremental rotations are formulated as,

$$\Delta\theta_{y1i} = \Delta\alpha_{y1i} + \Delta\beta_{yi} \tag{55}$$

$$\Delta\theta_{y2i} = \Delta\alpha_{y2i} + \Delta\beta_{yi} \tag{56}$$

$$\Delta\theta_{z1i} = \Delta\alpha_{z1i} - \Delta\beta_{zi} \tag{57}$$

$$\Delta\theta_{z2i} = \Delta\alpha_{z2i} - \Delta\beta_{zi} \tag{58}$$

in which, $\Delta\alpha_{y1i}$, $\Delta\alpha_{y2i}$, $\Delta\alpha_{z1i}$ and $\Delta\alpha_{z2i}$ are the incremental rotations about the last known configuration; and $\Delta\beta_{yi}$ and $\Delta\beta_{zi}$ are the incremental rigid body rotations given by,

$$\Delta\beta_{yi} = \frac{\Delta w_{2i} - \Delta w_{1i}}{L_i} \tag{59}$$

$$\Delta\beta_{zi} = \frac{\Delta v_{2i} - \Delta v_{1i}}{L_i} \tag{60}$$

where, $L_i$ is the member length at the last known configuration; $\Delta w_{1i}$, $\Delta w_{2i}$, $\Delta v_{1i}$ and $\Delta v_{2i}$ are the displacements at member along local z- and y- axes respectively.

The relative incremental twist about the shear center can be simply evaluated as,

$$\Delta\theta_{xi} = \Delta\theta_{x2i} - \Delta\theta_{x1i} \tag{61}$$

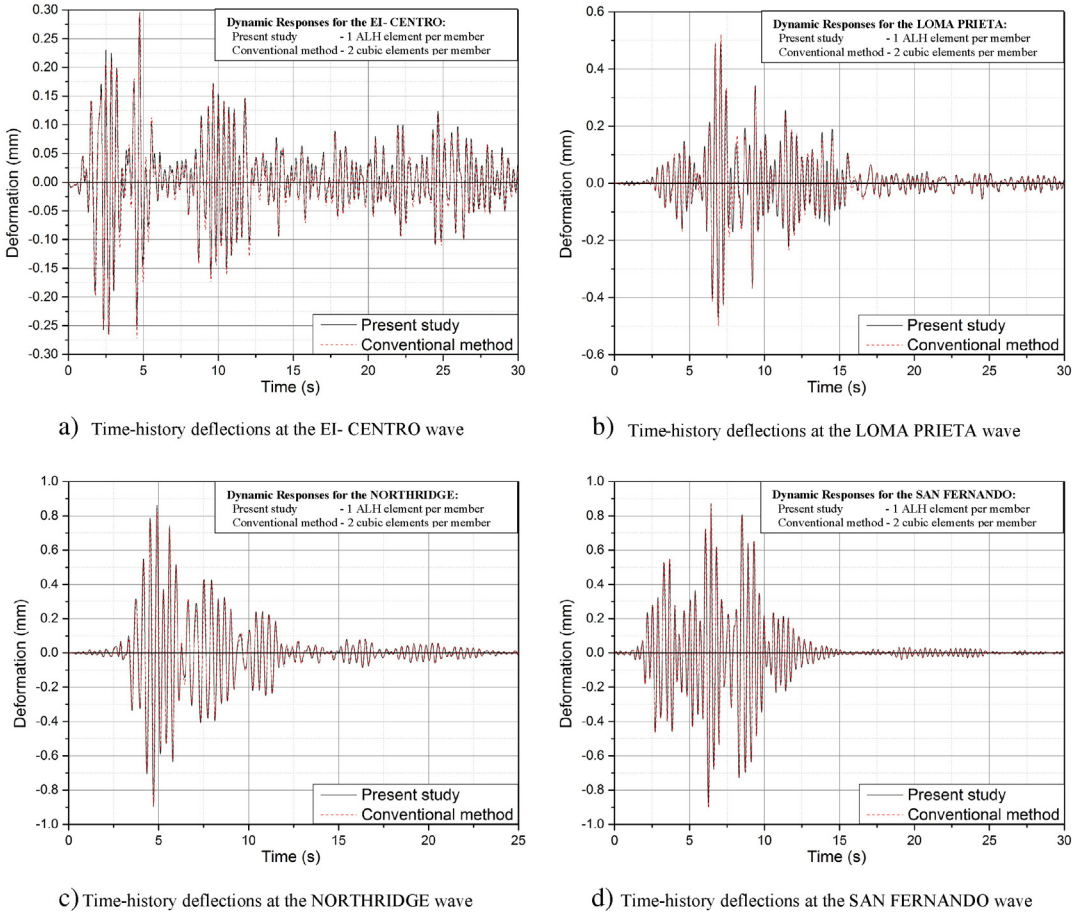


**Fig. 8.** Dynamic response analysis results of the 3D frame.

Please cite this article as: Liu S-W, et al, Dynamic Time-history Elastic Analysis of Steel Frames Using One Element per Member, Structures (2016), http://dx.doi.org/10.1016/j.istruc.2016.05.006

The incremental axial lengthening can be determined as,

$$\Delta e_i = \Delta u_b - \Delta u_{ni} \tag{62}$$

where,

$$\Delta u_{ni} = L_{i+1} - L_i \tag{63}$$

and the $\Delta u_b$ can be obtained by the first deviation of the expressions of $u_b$.

## 6. Verification examples

Three examples are selected and presented in this section to validate the present numerical framework in simulating the dynamic responses of steel frames and members under the transient actions.

### 6.1. Example 1: dynamic response of a cantilever column

In order to verify and validate the accuracy of the numerical method, a cantilever steel column is introduced and analyzed by the proposed one-element-per-member model. The column is 10 meter height with one end fixed and one end free. Rectangular box section is assigned to the column, where the section width, height and wall thickness are 500 mm, 500 mm and 50 mm, respectively. The column is made by steel, and the Young's modulus and density are 205,000 MPa and 77 kN/m$^3$. The dynamic excitation is applied at the first 0.14 s, and given as below:

$$\frac{a(t)}{g} = \begin{cases} 1+50t & t \le 0.02s \\ 3-50t & 0.02s \le st \le 0.10s \\ -7+50t & 0.10s \le st \le 0.14s \\ 0 & t \ge 0.14s \end{cases} \tag{64}$$

in which, $a(t)$ is the ground acceleration; $g$ is the gravity acceleration; and $t$ is the time.

The time increment for the analysis is 0.02 s, and the total time is set to be 10 s to examine the freely vibrated behaviors of the column after the excitation is withdrawn. The Newmark's coefficients $\gamma$ and $\beta$ are taken as 0.5 and 0.25, respectively. Also, the parameters from the Eqs (34) to (39) are calculated accordingly as: $c_1 = 10{,}000$, $c_2 = -200$, $c_3 = -2$, $c_4 = 100$, $c_5 = -2$ and $c_6 = 0$.

The conventional methods, using one, two or four elements to simulate a single member, are employed for comparisons, plotting in Fig. 4(a) to (c). The results from the proposed algorithm are closed to those from the models using 2 and 4 cubic elements per member. Further, the errors are apparent when using one cubic element to simulate a member. However, the results from those generated by 2 and 4 cubic elements per member models are closed, indicating at least 2 or more elements are required to model one member in the conventional method using the cubic element. Consequentially, the results verify the analysis accuracy of the proposed method in handling the highly nonlinear dynamic problem.

### 6.2. Example 2: time-history analysis of the seven-story frame

In this example, the seven-story planar frame is selected, and analyzed by applying the dynamic excitation to the structure. Section assignments and dimensions of the frame are presented in Fig. 5, where the details for the section properties are tabulated in Table 1. The N–S component of El-Centro earthquake [29] wave is employed for the current study and applied at the +X direction as the transient motion. The Young's modulus and density are 205 GPa and 77 kN/m$^3$, respectively. The dynamic coefficients $a$ and $b$ are taken as 0.117 and 0.005, respectively. The Newmark's parameters are $c_1 = 160{,}000$, $c_2 = -800$, $c_3 = -2$, $c_4 = 400$, $c_5 = -2$ and $c_6 = 0$. The deflection of the node number as 24 (see Fig. 5(b)) in the X direction is recorded and plotted in Fig. 6.

The conventional approach using the two cubic elements per member modeling method is introduced for comparisons, and those results are shown in Fig. 6. The results clearly indicate the satisfactory performance of the proposed numerical framework, where the curves from the two approaches are mostly identical. It also shows the significant reduction on computation expense and memory storage. For example, the matrix sizes for the proposed and the conventional models are $144 \times 144$ and $324 \times 324$, respectively, and therefore, the saving in the calculation time can be approximately up to 80% when the current method is used.

### 6.3. Example 3: four-story 3D frame subjected to seismic excitations

This example employs a 3D multi-story steel frame with irregular layout for the current study, which is illustrated in Fig. 7. The section properties are given in Table 2. Four seismic waves are selected, e.g. the El-Centro (1940), the San Fernando waves (1971), the Loma Prieta (1989), and the Northridge (1994) [29]. The dynamic coefficients $a$ and $b$ are 0.092 and 0.0075, respectively, while the Newmark's parameters are given as: $c_1 = 40{,}000$, $c_2 = -400$, $c_3 = -2$, $c_4 = 200$, $c_5 = -2$ and $c_6 = 0$. The displacement at the node no. 30 at the X-direction is monitored and plotted from Fig. 8(a) to (d) for the different seismic waves.

From the analysis results, it shows that the structure exhibits highly nonlinear behaviors under the seismic excitations, where large global deflections and member deformations are observed. The example confirms the validity of the present method in investigating the dynamic behaviors of the steel space frames and members under the transient actions.

## 7. Conclusions

This paper presents an efficient numerical analysis framework for the dynamic time-history elastic analysis of three-dimensional steel frames using one-element-per-member model. The curved arbitrarily-located-hinge (ALH) beam-column element is employed for simulating structural members, which is especially developed for the second-order design of steel frames fulfilled to the requirements in modern design codes like Eurocode 3 [12] and AISC 2010 [30] and so on. For improving the numerical efficiency, the internal DOFs are condensed. The present research focuses on studying the elastic behaviors of the system, while geometric nonlinearly, e.g. P-Δ-δ effects, large global deflections and local member deformations, are considered in the analysis. Consistent element mass matrix utilizing the Hemite interpolation function is proposed, and the Rayleigh damping model is employed. To solve the step-by-step equation to the dynamic motions, a direct time-integration method by the Newmark's algorithm is chosen. In describing the kinematic motion, the incremental secant stiffness method is introduced for allowing arbitrarily large rotations. Finally, several verification examples are given to verify and validate the presented numerical framework for solving dynamic time-integration problems. This research integrates the high-performance element into a robust numerical framework, and therefore, saving in the computational expense is apparent to make the current method being practical for practice.

## Acknowledgments

The authors are grateful to the financial supports by the Research Grant Council of the Hong Kong SAR Government on the project "Second-order and Advanced Analysis of Steel Frames Second-order and Advanced Analysis of Arches and Curved Structures (PolyU 152012/14E)" and "Second-Order Analysis of Flexible Steel Cable Nets Supporting Debris (PolyU 152008/15E)" and The Hong Kong Polytechnic University for the project "Stability Design of Composite Structures by Direct Analysis". This first author would like to appreciate the financial support by the Faculty of Construction and Environment through the project "FCE Postdoctoral Fellow Scheme".

Please cite this article as: Liu S-W, et al, Dynamic Time-history Elastic Analysis of Steel Frames Using One Element per Member, Structures (2016), http://dx.doi.org/10.1016/j.istruc.2016.05.006

## Appendix I. Secant relations

The secant relations for the curved ALH element without plastic deformations are given as below:

$$\begin{aligned}P = {} & \frac{EA}{L}e + \frac{12EA}{5L^2}{\delta_y}^2 + \frac{12EA}{5L^2}{\delta_z}^2 + \frac{EA}{30}{\theta_{11y}}^2 + \frac{EA}{30}{\theta_{11z}}^2 + \left(-\frac{EA}{6L}v_{m0y} - \frac{EA}{10L}\delta_z\right)\theta_{12y} \\ & + \frac{EA}{30}{\theta_{12y}}^2 + \theta_{11y}\left(\frac{EA}{6L}v_{m0y} - \frac{EA}{10L}\delta_z - \frac{EA}{60}\theta_{12y}\right) + \left(-\frac{EA}{6L}v_{m0z} - \frac{EA}{10L}\delta_y\right)\theta_{12z} \\ & + \frac{EA}{30}{\theta_{12z}}^2 + \theta_{11z}\left(\frac{EA}{6L}v_{m0z} - \frac{EA}{10L}\delta_y - \frac{EA}{60}\theta_{12z}\right) + \frac{EA}{30}{\theta_{21y}}^2 + \frac{EA}{30}{\theta_{21z}}^2 \\ & - \frac{EA}{6L}v_{m0y}\theta_{22y} + \frac{EA}{30}{\theta_{22y}}^2 + \theta_{21y}\left(\frac{EA}{6L}v_{m0y} - \frac{EA}{60}\theta_{22y}\right) \\ & + \delta_z\left(\frac{4EA}{L^2}v_{m0y} + \frac{EA}{10L}\theta_{21y} + \frac{EA}{10L}\theta_{22y}\right) - \frac{EA}{6L}v_{m0z}\theta_{22z} + \frac{EA}{30}{\theta_{22z}}^2 \\ & + \theta_{21z}\left(\frac{EA}{6L}v_{m0z} - \frac{EA}{60}\theta_{22z}\right) + \delta_y\left(\frac{4EA}{L^2}v_{m0z} + \frac{EA}{10L}\theta_{21z} + \frac{EA}{10L}\theta_{22z}\right)\end{aligned} \tag{65}$$

$$\begin{aligned}M_{11y} = {} & \frac{8EI_y}{L}\theta_{11y} + \frac{4EI_y}{L}\theta_{12y} - \frac{24EI_y}{L^2}\delta_z + \frac{LP}{15}\theta_{11y} - \frac{LP}{60}\theta_{12y} - \frac{P}{10}\delta_z \\ & + \frac{P}{6}v_{m0y}\end{aligned} \tag{66}$$

$$\begin{aligned}M_{11z} = {} & \frac{8EI_z}{L}\theta_{11z} + \frac{4EI_z}{L}\theta_{12z} - \frac{24EI_z}{L^2}\delta_y + \frac{LP}{15}\theta_{11z} - \frac{LP}{60}\theta_{12z} - \frac{P}{10}\delta_y \\ & + \frac{P}{6}v_{m0z}\end{aligned} \tag{67}$$

$$\begin{aligned}M_{12y} = {} & \frac{4EI_y}{L}\theta_{11y} + \frac{8EI_y}{L}\theta_{12y} - \frac{24EI_y}{L^2}\delta_z - \frac{LP}{60}\theta_{11y} \\ & + \frac{LP}{15}\theta_{12y} - \frac{P}{10}\delta_z - \frac{P}{6}v_{m0y}\end{aligned} \tag{68}$$

$$\begin{aligned}M_{12z} = {} & \frac{4EI_z}{L}\theta_{11z} + \frac{8EI_z}{L}\theta_{12z} - \frac{24EI_z}{L^2}\delta_y - \frac{LP}{60}\theta_{11z} \\ & + \frac{LP}{15}\theta_{12z} - \frac{P}{10}\delta_y - \frac{P}{6}v_{m0z}\end{aligned} \tag{69}$$

$$\begin{aligned}F_z = {} & \frac{24EI_y}{L^3}\left[8\delta_z + L(-\theta_{11y} - \theta_{12y} + \theta_{21y} + \theta_{22y})\right] \\ & + \frac{P}{10L}\left[48\delta_z + L(-\theta_{11y} - \theta_{12y} + \theta_{21y} + \theta_{22y}) + 40v_{m0y}\right]\end{aligned} \tag{70}$$

$$\begin{aligned}F_y = {} & \frac{24EI_z}{L^3}\left[8\delta_y + L(-\theta_{11z} - \theta_{12z} + \theta_{21z} + \theta_{22z})\right] \\ & + \frac{P}{10L}\left[48\delta_y + L(-\theta_{11z} - \theta_{12z} + \theta_{21z} + \theta_{22z}) + 40v_{m0z}\right]\end{aligned} \tag{71}$$

$$\begin{aligned}M_{21y} = {} & \frac{8EI_y}{L}\theta_{21y} + \frac{4EI_y}{L}\theta_{22y} + \frac{24EI_y}{L^2}\delta_z + \frac{LP}{15}\theta_{21y} - \frac{LP}{60}\theta_{22y} + \frac{P}{10}\delta_z \\ & + \frac{P}{6}v_{m0y}\end{aligned} \tag{72}$$

$$\begin{aligned}M_{21z} = {} & \frac{8EI_z}{L}\theta_{21z} + \frac{4EI_z}{L}\theta_{22z} + \frac{24EI_z}{L^2}\delta_y + \frac{LP}{15}\theta_{21z} - \frac{LP}{60}\theta_{22z} + \frac{P}{10}\delta_y \\ & + \frac{P}{6}v_{m0z}\end{aligned} \tag{73}$$

$$\begin{aligned}M_{22y} = {} & \frac{4EI_y}{L}\theta_{21y} + \frac{8EI_y}{L}\theta_{22y} + \frac{24EI_y}{L^2}\delta_z - \frac{LP}{60}\theta_{21y} + \frac{LP}{15}\theta_{22}y \\ & + \frac{P}{10}\delta_z - \frac{P}{6}v_{m0y}\end{aligned} \tag{74}$$

$$\begin{aligned}M_{22z} = {} & \frac{4EI_z}{L}\theta_{21z} + \frac{8EI_z}{L}\theta_{22z} + \frac{24EI_z}{L^2}\delta_y - \frac{LP}{60}\theta_{21z} + \frac{LP}{15}\theta_{22z} \\ & + \frac{P}{10}\delta_y - \frac{P}{6}v_{m0z}\end{aligned} \tag{75}$$

$$M_t = \frac{GJ}{L}\theta_x \tag{76}$$

## References


[1] Nguyen DT. Finite element methods: parallel-sparse statics and Eigen-solutions. Springer Science & Business Media; 2006.
[2] Nader M, Astaneh A. Dynamic behavior of flexible, semirigid and rigid steel frames. J Constr Steel Res 1991;18(3):179–92.
[3] Chui PPT, Chan SL. Transient response of moment-resistant steel frames with flexible and hysteretic joints. J Constr Steel Res 1996;39(3):221–43.
[4] Awkar J, Lui E. Seismic analysis and response of multistory semirigid frames. Eng Struct 1999;21(5):425–41.
[5] Chan SL, Chui PT. Non-linear static and cyclic analysis of steel frames with semi-rigid connections. Elsevier; 2000.
[6] Gupta A, Krawinkler H. Dynamic P-delta effects for flexible inelastic steel structures. J Struct Eng 2000;126(1):145–54.
[7] Foutch DA, Yun SY. Modeling of steel moment frames for seismic loads. J Constr Steel Res 2002;58(5–8):529–64.
[8] Ohtori Y, Christenson R, Spencer Jr B, Dyke S. Benchmark control problems for seismically excited nonlinear buildings. J Eng Mech 2004;130(4):366–85.
[9] Da Silva J, De Lima L, Vellasco PdS, De Andrade S, De Castro R. Nonlinear dynamic analysis of steel portal frames with semi-rigid connections. Eng Struct 2008;30(9):2566–79.
[10] Nguyen PC, Kim SE. Nonlinear elastic dynamic analysis of space steel frames with semi-rigid connections. J Constr Steel Res 2013;84:72–81.
[11] The European Committee for Standardization (CEN). Eurocode 8–design of structures for earthquake resistance–part 1: general rules, seismic actions and rules for buildings. European standard NF EN; 1998. p. 1.
[12] The European Committee for Standardization (CEN). Eurocode 3: design of steel structures: part 1-1: general rules and rules for buildings; 2005.
[13] Chan SL, Zhou ZH. Pointwise equilibrating polynomial element for nonlinear-analysis of frames. J Struct Eng ASCE 1994;120(6):1703–17.
[14] Chan SL, Gu JX. Exact tangent stiffness for imperfect beam-column members - closure. J Struct Eng ASCE 2001;127(12):1492–4.
[15] Liu SW, Liu YP, Chan SL. Direct analysis by an arbitrarily-located-plastic-hinge element — part 2: spatial analysis. J Constr Steel Res 2014;103:316–26.
[16] Liu SW, Liu YP, Chan SL. Direct analysis by an arbitrarily-located-plastic-hinge element — part 1: planar analysis. J Constr Steel Res 2014;103:303–15.
[17] Bathe KJ. Finite element procedures. Klaus-Jurgen Bathe; 2006.
[18] Newmark NM. A method of computation for structural dynamics. J Eng Mech Div 1959;85(3):67–94.
[19] Liu M, Gorman D. Formulation of Rayleigh damping and its extensions. Comput Struct 1995;57(2):277–85.
[20] Chan SL. Large deflection kinematic formulations for three-dimensional framed structures. Comput Methods Appl Mech Eng 1992;95(1):17–36.
[21] So AKW, Chan SL. Buckling and geometrically nonlinear analysis of frames using one element/member. J Constr Steel Res 1991;20(4):271–89.
[22] Ho GWM, Chan SL. An accurate and efficient method for large deflection inelastic analysis of frames with semi-rigid connections. J Constr Steel Res 1993;26(2):171–91.
[23] Liu SW, Liu YP, Chan SL. Advanced analysis of hybrid steel and concrete frames: part 1: cross-section analysis technique and second-order analysis. J Constr Steel Res 2012;70:326–36.
[24] Liu SW, Liu YP, Chan SL. Advanced analysis of hybrid steel and concrete frames: part 2: refined plastic hinge and advanced analysis. J Constr Steel Res 2012;70:337–49.
[25] Chan SL. Large deflection dynamic analysis of space frames. Comput Struct 1996;58(2):381–7.
[26] Chan SL. Large deflection kinematic formulations for 3-dimensional framed structures. Comput Methods Appl Mech Eng 1992;95(1):17–36.
[27] Yang YB, Chiou HT. Rigid body motion test for nonlinear analysis with beam elements. J Eng Mech 1987;113(9):1404–19.
[28] Argyris J. An excursion into large rotations. Comput Methods Appl Mech Eng 1982;32(1):85–155.
[29] Council, Building Seismic Safety. NEHRP recommended provisions: design examples. National Institute of Building Sciences; 2006.
[30] American Institute of Steel Construction. In: A.I.o.S. Construction, editor. Specification for structural steel buildings. American Institute of Steel Construction; 2010.


Please cite this article as: Liu S-W, et al, Dynamic Time-history Elastic Analysis of Steel Frames Using One Element per Member, Structures (2016), http://dx.doi.org/10.1016/j.istruc.2016.05.006